Fundamental limit of bandwidth-extrapolation-based superresolution

Yunkai Wang [*] and Virginia O. Lorenz
IQUIST, University of Illinois Urbana-Champaign, Urbana, Illinois 61801, USA
and Department of Physics, University of Illinois Urbana-Champaign, Urbana, Illinois 61801, USA

(Received 19 December 2022; revised 26 February 2023; accepted 23 May 2023; published 5 July 2023)

Here we relate two methods of subdiffraction imaging: bandwidth extrapolation for spatially bounded sources and quantum-metrology-inspired methods under assumptions about source structure. We present a quantum estimation theoretical approach in which the source is modeled in terms of unknown parameters corresponding to the Fourier components, whose impact on resolution is very intuitive. Using this method, we find that imaging spatially bounded sources faces an unavoidable fundamental resolution limit, but that in the small-source limit, certain measurement approaches can significantly improve the sensitivity over conventional methods.

DOI: 10.1103/PhysRevA.108.012602

I. INTRODUCTION

Imaging resolution is limited by diffraction when light from the source encounters an imaging system with finite size. This is because a finite-size imaging system introduces a cutoff in the spatial spectrum of the image, capturing only a finite portion of the object's Fourier spectrum. However, the Fourier spectrum of a spatially bounded source is an analytical function, which means we can take advantage of the mathematical method of analytical continuation in which an entire analytical function can be determined using knowledge of a small but finite region of the function. This means knowing a finite portion of the spectrum of a spatially bounded object is enough to obtain the whole spectrum by analytical continuation. Indeed, it is known that for spatially bounded objects, resolution beyond the diffraction limit is theoretically possible [1–5].

More intuitively, if we consider a spatially bounded source as shown in Fig. 1, a finite-size lens produces a Fourier transformation of the source's intensity distribution $I(u)$ as its spectrum $g(k) = \int du\, I(u) e^{iku}$, where k is the spatial frequency. Regarding the spectrum $g(k)$ as a function of spatial frequency k, we call $g(k)$ high (low)-frequency information for relatively large (small) $|k|$. The finite size of the imaging system introduces a cutoff $k_0 > 0$ in the spectrum, beyond which higher information $g(k)$ with $|k| > k_0$ is lost. The tails on the low-frequency side of the cutoff with $|k| < k_0$ are related to the Fourier components on the high-frequency side of the cutoff with $|k| > k_0$ and can be measured from them. This is sometimes referred to as superresolution; in the field of Fourier optics it is called bandwidth extrapolation, which is the term we employ here to distinguish it from other methods of subdiffraction imaging. There are several ways to extract the high-frequency information, including analytical constructions [1–3] and iterative methods designed for digital data processing [6,7]. Nevertheless, the limitation of the bandwidth extrapolation method is clear: The mathematical theorem relies on the assumption that the function can be known with infinite accuracy in a finite region, which is not realistic in real-world applications. A common way to gain the high-spatial-frequency information is to relate the high-frequency components to the low-frequency components using a set of linear equations. The coefficient matrix of the equation set is ill-conditioned because the spatial frequency components beyond the cutoff are only weakly related to the measured low-frequency information. When the high-frequency information is calculated by reversing the coefficient matrix, it is strongly degraded by any noise in the measured low-frequency information [4,8,9].

Another line of effort for subdiffraction imaging is inspired by quantum estimation theory. Methods in this area are also usually described as superresolution, but here we refer to them as quantum-metrology-inspired methods to distinguish from bandwidth extrapolation. This topic was initiated by a very interesting discovery that, in measuring the separation between two weak incoherent point sources of equal intensity in one dimension, Rayleigh's limit in resolving two point sources can be avoided [10,11]. This discovery was made by regarding the problem of resolving two point sources as a problem of estimating unknown parameters, in this case the separation. To determine the unknown parameters, states that depend on the unknown parameters are measured. Quantum estimation theory is used to quantify the sensitivity of measuring the unknown parameters, calculated as a quantity called the Fisher information (FI) [12], which is defined in terms of the derivative of the probability distribution of a measurement over the unknown parameters. Intuitively, the probability can be regarded as the measured signal, with larger FI indicating that the measured signal is more sensitive to the parameters we want to estimate. Mathematically, the inverse of the FI is a lower bound of the variance of estimating the unknown parameters using certain estimation strategies. Since the FI is defined for a particular measurement, we want to optimize over all possible measurement instruments and strategies to obtain the largest FI. It turns out the FI optimized for all

[*] yunkaiw2@illinois.edu

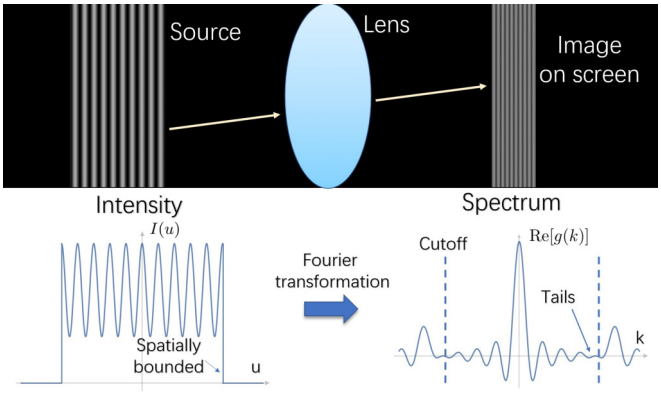

FIG. 1. Example of imaging a spatially bounded source with an imaging system of finite size. The intensity distribution of the source object is $I(u) = [1 + m\cos(\pi u)]/20$, which is nonvanishing only within $-10 \leqslant u \leqslant 10$, and $m = \frac{1}{2}$ is the high-frequency information of the source we want to measure. The spectrum of the original intensity distribution is $g(k) = \int du\, I(u) e^{iku}$ and we plot the real part of $g(k)$ as a function of k. The dashed vertical lines show the spectrum cutoffs due to the finite size of the imaging system. The amplitudes of the high-frequency components are related to m but outside the cutoffs of the spectrum. However, since the source is spatially bounded, the tails on the low-frequency side of the cutoffs contain information about the high-frequency components. Bandwidth extrapolation corresponds to measuring the tails within the spectrum cutoffs to obtain the high-frequency information.

possible measurements can be calculated directly from the state that depends on the unknown parameters without referring to any specific measurement. This calculated value is known as the quantum Fisher information (QFI) [13,14] and gives a fundamental bound for imaging quality.

Although the model of two point sources with equal intensity comprises a simple imaging problem for determining resolution limits and exhibits new possibilities for improving imaging quality, this system is not of great practical interest, so much effort has been made to consider more general source cases. Because the analysis of quantum-metrology-inspired methods relies on quantum estimation theory, these results usually assume the sources have some structure described by some unknown parameters, such as the coordinates of point sources. Point sources with unequal or stronger intensity [15–19] and point sources in two or three dimensions [20–23] have been considered. Applying quantum-metrology-inspired methods to general extended sources has been discussed so far in Refs. [24–26]. These discussions model general extended sources using moments as the set of parameters; nth-order moments x_n are defined as the mean value $\langle u^n \rangle$ averaged over the intensity distribution $I(u)$, where u is the coordinate on the object plane and n is a nonnegative integer. Compared to the use of Fourier components, the variance of estimating moments does not have as direct an interpretation in terms of resolution or imaging quality.

From the above it is clear that bandwidth extrapolation and quantum-metrology-inspired methods are based on different principles. Bandwidth extrapolation relies on the fact that high-frequency information beyond the cutoff of the imaging system is weakly related to the low-frequency information under the assumption of spatially bounded sources. Quantum-metrology-inspired methods systematically optimize the measurement using quantum estimation theory. It is very tempting to ask if there is a relation between these approaches. For example, if more carefully designed measurement can improve the sensitivity of estimating certain parameters in the quantum-metrology-inspired methods, can this help us improve the quality of images reconstructed in bandwidth extrapolation and if so, how? We can also interpret quantum-metrology-inspired methods based on ideas from bandwidth extrapolation. Most of the source structures that have been studied in quantum-metrology-inspired methods are spatially bounded, which means fine details such as the separation between two point sources can be inferred from the low-frequency information.

We clarify here the relation between these two methods by applying quantum estimation theory to bandwidth extrapolation for a simple example of a source with two high-frequency Fourier components a and b, which are directly related to $\pm g(k_{1,2})$ at spatial frequencies $k_{1,2}$, respectively, as detailed in Appendix A. It turns out that a low-frequency Fourier component g can be related to the high-frequency terms using a linear equation $g = e^{i\phi}(\mathrm{sinc}\alpha + Aa + iBb)$, which will be derived in detail later. This relation allows us to infer a and b from g. However, the high-frequency terms have very small prefactors A and B. This gives a small QFI of estimating the two high-frequency Fourier components a and b, which means the fundamental lower bound of the variance of the estimation with any quantum measurement is very large. We calculate the FI of estimating the two high-frequency Fourier components a and b with a fixed phase measurement. We then compare the QFI and FI of a fixed phase measurement in two interesting limiting cases. The first case is the small-source limit corresponding to the whole size of the source being much smaller than the resolution limit. Although the estimation of high-frequency terms is fundamentally hard, as predicted by the QFI, by comparing the FI of the fixed phase measurement with the QFI, we find that in the limit of small sources there is still much room for improvement. We also construct a measurement strategy with an increased FI in the small-source limit. The second case we consider is when the size of the source is larger than the resolution limit but we hope to measure the fine details of the source that are much smaller than the resolution limit. Although there is no discovered improvement, our discussion allows better understanding of this limiting case, which has not been carefully considered in previous work in quantum-metrology-inspired methods. The discussion in the simple case of two high-frequency Fourier components suggests potential advantages when there are more than two Fourier components. We end by reinterpreting quantum-metrology-inspired methods using bandwidth extrapolation.

II. BANDWIDTH EXTRAPOLATION PROBLEM REVISITED WITH QUANTUM ESTIMATION THEORY

In this section we discuss the connections between bandwidth extrapolation and quantum-metrology-inspired methods for interferometric imaging using a simple example of a source with only two spatial frequencies. We choose to

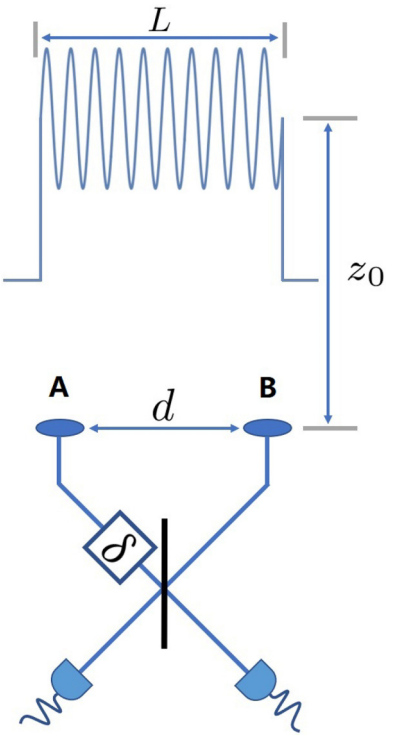

FIG. 2. Interferometer with two detectors used for measuring low-frequency Fourier components of the source. Here L is the size ofthe source, d is the length of the baseline, z_0 is the distance from the source to the collection apertures A and B, and δ is the controllable phase delay added in the measurement.

focus on interferometric imaging due to its direct connection to Fourier optics and hence bandwidth extrapolation. In the limit of a large number of baselines, the interferometer array can also effectively be regarded as a single lens, making single-lens imaging a special case. We use quantum estimation theory to derive the fundamental limit of estimating the high-frequency Fourier components beyond the cutoff, which is the key idea of the bandwidth extrapolation method. We start with a simple example, shown in Fig. 2, to demonstrate the basic idea of how the estimation of high-spatial-frequency information beyond the resolution of the imaging system is affected when a measurement is designed more carefully based on quantum estimation theory. Throughout this work, we consider thermal sources in the weak limit. We assume the sources are monochromatic and that the radiation from different points on the sources is incoherent. A source in one dimension that has intensity oscillating with position is similar to what we show in Fig. 1, which can be described with the spatially bounded intensity distribution

$$I(u) = \left(\frac{1}{L} + \frac{a}{L}\cos k_1(u-u_0) + \frac{b}{L}\sin k_2(u-u_0)\right)\mathrm{rect}(u),$$
$$\mathrm{rect}(u) = \begin{cases} 1 & \text{for } u_0 - \frac{L}{2} \leqslant u \leqslant u_0 + \frac{L}{2} \\ 0 & \text{otherwise,} \end{cases} \tag{1}$$

where u is the coordinate on the object plane, L is the upper bound of the size of the source, $k_1 = 2\pi n_1/L$ and $k_2 = 2\pi n_2/L$ are the spatial frequencies, n_1 and n_2 are nonzero integers (we will consider noninteger $n_{1,2}$ later on), u_0 is the centroid of the source, and a and b are the unknown parameters we want to measure and are directly related to $g(\pm k_{1,2})$, respectively, as detailed in Appendix A. Note that, in practice, a and b can only have values such that $I(u) \geqslant 0$ for any u. By choosing this form of $I(u)$, the intensity distribution is already normalized, i.e., $\int du\, I(u) = 1$. Note that $k_{1,2}$ can be assumed to be known and we only need to measure a and b. This is because we can apply the Whittaker-Shannon sampling theorem for spatially bounded sources [4], which says that we only need to measure the Fourier components at a discrete set of spatial frequencies to image a spatially bounded source without losing any information. In addition, we have the freedom to choose this discrete set of spatial frequencies, which means these spatial frequencies are known in advance. We give detailed derivations for this argument in Appendix A. Nevertheless, in case it is still desirable to consider $k_{1,2}$ as unknown parameters, we discuss methods to do so later on.

We consider imaging this source with an interferometer (Fig. 2), where light from the source is collected into two spatial modes labeled A and B corresponding to two collection apertures A and B separated by a baseline d, which are the basic components of interferometric imaging. In the weak-source and far-field limit, after postselecting on detection of one photon, written in the single-photon basis states $|1_A 0_B\rangle$ and $|0_A 1_B\rangle$ at the two spatial modes, the density matrix of the state received by the two spatial modes is [27]

$$\rho = \frac{1}{2}\begin{bmatrix} 1 & g \\ g^* & 1 \end{bmatrix}, \tag{2}$$

where g is the coherence function, which is a Fourier component of the source. We now derive g as an explicit function of the baseline, whose length d is limited in practice. For convenience of discussion, we first define

$$\alpha = \frac{dL\omega}{2cz_0}, \tag{3}$$

where ω is the frequency of the light, c is the speed of light, and z_0 is the distance between the imaging plane and the source plane. Notice that the resolution limit of the interferometer with baseline d is roughly $\frac{2cz_0}{d\omega}$, which means α is the ratio between the upper bound of the size of the source L and the resolution limit of the interferometer. We can then calculate the coherence function based on the van Cittert–Zernike theorem as [28]

$$g = \int du\, I(u) \exp\left(i\frac{\omega}{c}\frac{ud}{z_0}\right) = e^{i\phi}(\mathrm{sinc}\alpha + Aa + iBb), \tag{4}$$

where $\phi = \frac{\omega}{c}\frac{u_0 d}{z_0}$, $\mathrm{sinc}\alpha = \frac{\sin\alpha}{\alpha}$, and the coefficients

$$A = (-1)^{n_1}\frac{\alpha\sin\alpha}{\alpha^2 - n_1^2\pi^2} = \frac{1}{2}[\mathrm{sinc}(\alpha - n_1\pi) + \mathrm{sinc}(\alpha + n_1\pi)],$$
$$B = (-1)^{n_2}\frac{n_2\pi\sin\alpha}{\alpha^2 - n_2^2\pi^2} = \frac{1}{2}[\mathrm{sinc}(\alpha - n_2\pi) - \mathrm{sinc}(\alpha + n_2\pi)]. \tag{5}$$

We can observe that g is actually the Fourier component at spatial frequency $\omega d/cz_0$. Any pair of points on the image plane can be used to measure one Fourier component $g(k)$

with spatial frequency $k = \omega d/cz_0$ determined by their baseline d. However, note that although Eq. (4) is the Fourier component at frequency $\omega d/cz_0$, it contains information about a and b, which are the Fourier components at other frequencies k_1 and k_2. This is because the size of the source is limited within $u_0 - \frac{L}{2} \leqslant u \leqslant u_0 + \frac{L}{2}$ with a finite L, which means α is not infinity and A and B are nonvanishing. We can thus measure a and b even though we are measuring at a different spatial frequency, which is the basic spirit of bandwidth extrapolation. As we will see, we can analyze the performance predicted by the QFI using such intuition from the bandwidth extrapolation method. In particular, if the spatial frequencies k_1 and k_2 are much larger than $\omega d/cz_0$, which implies $\alpha \ll n_{1,2}\pi$ and hence $A, B \ll 1$, the variance of estimating a and b will be enlarged since g is linear in $Aa + Bb$. For the case of the source having many unknown Fourier components, this result indicates there will be a set of linear equations with small prefactors, which ultimately result in an ill-conditioned coefficient matrix when solving for the high-frequency information from the measured low-frequency information.

We now determine the fundamental limit of estimating the Fourier components a and b and find the measurement to approach this limit by making a connection to quantum-metrology-inspired methods, which rely on quantum estimation theory to determine the optimal sensitivity for any possible positive-operator-valued measure (POVM). More concretely, the fundamental limit of the variance of estimating unknown parameters $\vec{x} = [x_1, x_2, \ldots, x_n]^T$ can be calculated from the QFI [13,14], i.e., $\Sigma_{\vec{x}} \geqslant K^{-1}$, which is usually referred to as the quantum Cramér-Rao bound, where $[\Sigma_{\vec{x}}]_{ij} = \mathbb{E}[(x_i - \check{x}_i)(x_j - \check{x}_j)]$ is the (i, j) element, with $\check{x}_i$ the unbiased estimator of the ith unknown parameter. We calculate the QFI with the state given in Eq. (2), which is a single-photon state after postselection of one photon from thermal sources in the weak limit. Thus, we derive the QFI per source photon here. The QFI can be calculated from the symmetric logarithmic derivatives (SLDs), i.e., $K_{ij} = \mathrm{tr}(\mathcal{L}_i \mathcal{L}_j \rho)$, where the SLDs $\mathcal{L}_i$ can be calculated from the spectrum of the density matrix

$$\mathcal{L}_i = \sum_{\mu,\nu;D_\mu+D_\nu\neq 0} \frac{2}{D_\mu + D_\nu} \langle e_\mu| \frac{\partial \rho}{\partial x_i} |e_\nu\rangle |e_\mu\rangle \langle e_\nu|, \quad (6)$$

where $|e_\mu\rangle$ is the eigenbasis of ρ of eigenvalue D_μ. In an imaging problem, we can estimate the Fourier component to obtain information about the source. For a source with intensity distribution given in Eq. (1), the Fourier components to be measured are a and b. We can then also formulate the model of bandwidth extrapolation as a parameter estimation problem similar to quantum-metrology-inspired methods. We now perform the QFI calculation for the estimation of a and b as a way to quantify the quality of the imaging. The density matrix can be written in terms of the spectral decomposition

$$\begin{aligned} \rho &= D_1 |e_1\rangle \langle e_1| + D_2 |e_2\rangle \langle e_2|, \\ D_1 &= \tfrac{1}{2}(1 - |g|), \quad |e_1\rangle = [-e^{i\theta}, 1]^T/\sqrt{2}, \\ D_2 &= \tfrac{1}{2}(1 + |g|), \quad |e_2\rangle = [e^{i\theta}, 1]^T/\sqrt{2}, \end{aligned} \quad (7)$$

where $g = |g|e^{i\theta}$ and $|e_{1,2}\rangle$ are written in basis states $|1_A 0_B\rangle$ and $|0_A 1_B\rangle$. We can then calculate SLDs

$$\begin{aligned} \mathcal{L}_a &= iA\sin(\theta-\phi)|e_1\rangle\langle e_2| - iA\sin(\theta-\phi)|e_2\rangle\langle e_1| \\ &\quad - \frac{A\cos(\theta-\phi)}{1-|g|}|e_1\rangle\langle e_1| + \frac{A\cos(\theta-\phi)}{1+|g|}|e_2\rangle\langle e_2|, \\ \mathcal{L}_b &= iB\cos(\theta-\phi)|e_2\rangle\langle e_1| - iB\cos(\theta-\phi)|e_1\rangle\langle e_2| \\ &\quad - \frac{B\sin(\theta-\phi)}{1-|g|}|e_1\rangle\langle e_1| + \frac{B\sin(\theta-\phi)}{1+|g|}|e_2\rangle\langle e_2|, \end{aligned} \quad (8)$$

whose eigenbasis gives the measurement that can saturate the QFI. The optimal POVM for estimating a is given by the projection onto the basis

$$\begin{aligned} |\psi_a\rangle &= [\pm ie^{i(\theta-\gamma_a)}, 1]/\sqrt{2}, \\ \gamma_a &= \arg[-i\cos(\phi-\theta) + (-1+|g|^2)\sin(\phi-\theta)]. \end{aligned} \quad (9)$$

The optimal POVM for estimating b is given by the projection onto the basis

$$\begin{aligned} |\psi_b\rangle &= [\pm ie^{i(\theta-\gamma_b)}, 1]/\sqrt{2}, \\ \gamma_b &= \arg[i\sin(\phi-\theta) + (-1+|g|^2)\cos(\phi-\theta)]. \end{aligned} \quad (10)$$

Note that ϕ, θ, and $|g|$ are unknown parameters, but to implement the optimal measurement designed here, we need to know them in advance. This is similar to the problem encountered in Ref. [10], in which prior knowledge is required about the centroid of two point sources to implement its proposed measurement. To implement the optimal measurement, the measurement can be performed adaptively to gradually approach the optimal measurement with more and more knowledge about these parameters. Furthermore, since the SLDs of a and b in Eq. (8) do not commute with each other, the two POVMs in Eqs. (9) and (10) are not compatible. These two measurements are only optimal for the estimation of parameter a or b alone. However, as pointed out in Refs. [29,30], even if the SLDs do not commute with each other, it is still possible to optimally estimate parameters simultaneously when the condition $\mathrm{tr}(\rho[\mathcal{L}_a, \mathcal{L}_b]) = 0$ is satisfied, where $[\mathcal{L}_a, \mathcal{L}_b] = \mathcal{L}_a\mathcal{L}_b - \mathcal{L}_b\mathcal{L}_a$. We can easily find this is indeed satisfied for the estimation of a and b even though the optimal measurement to estimate both of them might be collective over many copies of ρ, a topic beyond the scope of the present paper.

Result 1: Fundamental limit of bandwidth extrapolation for a simple source

The QFI K of estimating a and b for the intensity distribution in Eq. (1) with a two-spatial-mode interferometer array is derived to be

$$\begin{aligned} K_{aa} &= \mathrm{tr}(\mathcal{L}_a^2\rho) = A^2\frac{-2+|g|^2-|g|^2\cos(2\theta-2\phi)}{2(-1+|g|^2)}, \\ K_{bb} &= \mathrm{tr}(\mathcal{L}_b^2\rho) = B^2\frac{-2+|g|^2+|g|^2\cos(2\theta-2\phi)}{2(-1+|g|^2)}, \\ K_{ab} &= \mathrm{tr}(\mathcal{L}_a\mathcal{L}_b\rho) = AB\frac{|g|^2\sin(2\phi-2\theta)}{2(-1+|g|^2)}. \end{aligned} \quad (11)$$

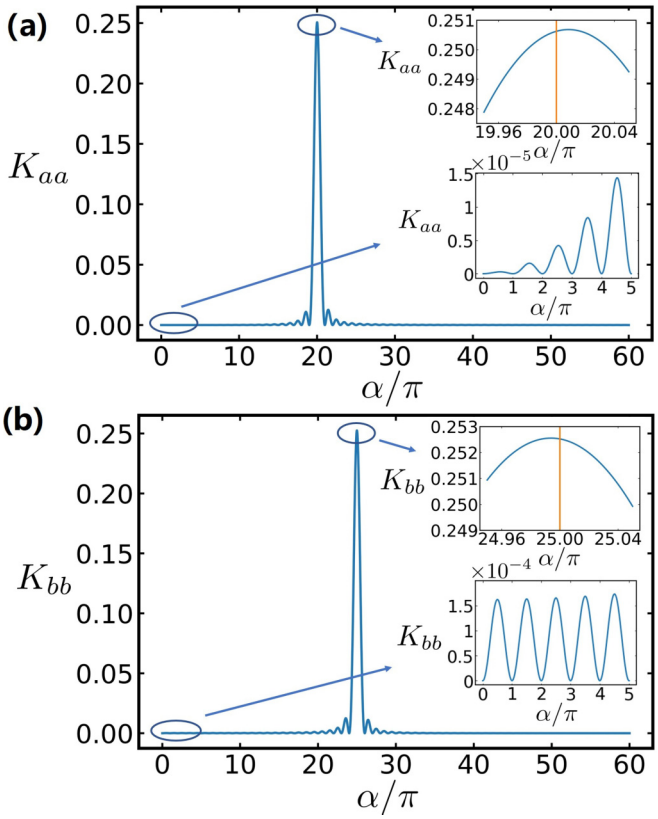

FIG. 3. Numerical calculation of the QFI (a) K_{aa} and (b) K_{bb} varying over α with $n_1 = 20$, $n_2 = 25$, $\phi = 0$, $a = 0.1$, and $b = 0.2$. The top insets in (a) and (b) concentrate on the peaks of K_{aa} and K_{bb}, whose maximal points slightly deviate from $\alpha = n_{1,2}\pi$. The bottom insets in (a) an (b) show K_{aa} and K_{bb} as $\alpha \to 0$. For this set of parameters, $K_{ab} < 2 \times 10^{-5}$ is very small and hence not plotted here.

The QFI depends on A and B, which is consistent with the intuition from bandwidth extrapolation. We choose representative parameters and plot the QFI of Eq. (11) in Fig. 3. The QFI exhibits oscillations with local maxima where α is an integer because for those values the measured Fourier component g times an integer gives the Fourier component we care about. We can see an overall trend that when α is close to $n_{1,2}\pi$, K_{aa} and K_{bb} approach their respective optimal values. This is reasonable because $\alpha = n_{1,2}\pi$ means the Fourier component g we are measuring exactly matches the Fourier component of interest. However, α is proportional to the baseline d of the interferometer, which is limited in practice. For baselines less than optimal, subdiffraction imaging corresponds to using the nonvanishing tail at smaller α, which enables estimating this information with a nonvanishing sensitivity and hence shows the bandwidth-extrapolation method can indeed measure the high-frequency information as promised. However, for small α, K_{aa} and K_{bb} are very small, which implies that the bandwidth extrapolation method fundamentally has very poor sensitivity even with the optimal quantum measurement.

The positions of maximal K_{aa} and K_{bb} actually slightly deviate from $\alpha = n_{1,2}\pi$, as shown in the top insets of Figs. 3(a) and 3(b). Mathematically, this arises from the $\mathrm{sinc}(\alpha + n_{1,2}\pi)$ terms of A and B in Eq. (5). These terms appear because

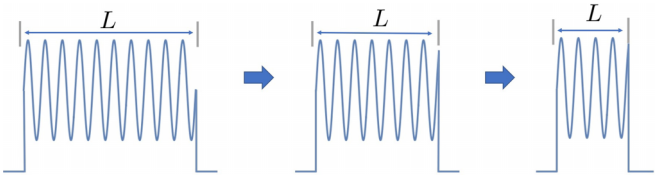

FIG. 4. Decreasing the size of the source L while fixing the spatial frequency $k_{1,2}$.

the intensity distribution of an incoherent source is described in terms of cosine or sine functions. In contrast, the coherence function is a Fourier component of a complex Fourier transformation of the intensity distribution. Thus, in practice, the interferometer baseline should slightly deviate from the frequency of the intensity oscillation of the source to achieve the best sensitivity. Typical real-world sources have a broader spatial spectrum than considered in this simplified model, so this small deviation may not be of much consequence in real-world applications.

We now analyze how the size of the source L affects the sensitivity, especially for the case where the longest baseline is not long enough to make $\alpha = n_{1,2}\pi$. One might immediately say that α is proportional to L, which means a larger source will give larger α, which will allow us to achieve better sensitivity. Since we are interested in resolving the fine details of the source, we fix the spatial frequencies $k_{1,2}$ and vary $n_{1,2}$ while varying L, as shown in Fig. 4; i.e., the size of the fine details are not affected while the whole size of the source varies. (If instead we fix $n_{1,2}$ and increase L, α also approaches $n_{1,2}\pi$ but the spatial frequencies $k_{1,2}$ are decreased, which means the fine details at these two frequencies are enlarged, which is not the situation of interest.) Note that as we fix $k_{1,2}$ and vary α, $n_{1,2}$ may not be integers, in which case $I(u)$ defined in Eq. (1) is no longer normalized, i.e., $\int du\, I(u) \neq 1$. So we renormalize $I(u) = [1 + a\cos k_1(u - u_0) + b\sin k_2(u - u_0)]\mathrm{rect}(u)/L(1 + a\mathrm{sinc}n_1\pi)$ by changing the prefactor and rederive the coherence function $g = e^{i\phi}(\mathrm{sinc}\alpha + Aa + iBb)/(1 + a\mathrm{sinc}n_1\pi)$ for renormalized $I(u)$. We include these considerations in the exact calculation below. We can analytically guess how the sensitivity of estimating these fine details is affected by considering Eqs. (5) and (11). The QFI is related to factors A^2, B^2, and AB and some other factors relevant to $|g|$ and θ. We will return to the factors related to $|g|$ and θ later in the limiting case $\alpha \to 0$ where they play an important role. Since the QFI is proportional to A^2, B^2, and AB, we now consider how A and B are affected upon varying L while fixing $k_{1,2}$. We know that $n_{1,2} = k_{1,2}L/2\pi$ and $\alpha = dL\omega/2cz_0$, so $n_{1,2} \propto L$ and $\alpha \propto L$. This immediately tells us from Eq. (5) that except for the oscillating term $\sin\alpha$, $A \propto L^{-1}$ and $B \propto L^{-1}$, which means the QFI $K_{aa,ab,bb} \propto L^{-2}$. In other words, a smaller source L actually leads to larger sensitivity. Intuitively, this is because for the same spatial frequency, when the source size becomes smaller, there is a larger deviation from the ideal single spatial frequency source, which means larger tails in the Fourier transformation and hence greater sensitivity for interferometers without high enough resolution. The above advantage does not persist if the size of the source becomes infinitely small, because the source must contain at least one period of oscillation, which is

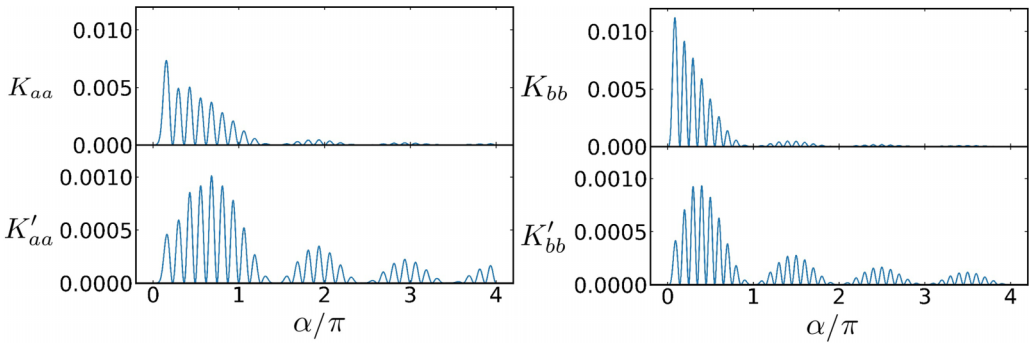

FIG. 5. Shown on top is the numerical calculation of QFI K_{aa} and K_{bb} varying over α with $\phi = 0$, $a = 0.1$, and $b = 0.2$. We fix the ratios $n_1\pi/\alpha = 8$ and $n_2\pi/\alpha = 10$ to fix the spatial frequency $k_{1,2}$. Shown on the bottom is the QFI K'_{aa} and K'_{bb} after multiplying K_{aa} and K_{bb} by the intensity to take into account the fact that smaller sources emit fewer photons and hence degrade the sensitivity. Without loss of generality, we have chosen the intensity at $\alpha = \frac{5}{2}\pi$ to be one.

the information we want to measure. As the source becomes smaller, even though there is a larger QFI $K_{aa,bb}$ per photon, there are fewer photons, which degrades the sensitivity. The total intensity of the source scales linearly with L (with some correction factor when $n_{1,2}$ are not integers). To be more concrete, we use the unnormalized intensity distribution $I(u) = I_0[1 + a\cos k_1(u-u_0) + b\sin k_2(u-u_0)]\mathrm{rect}(u)$, where I_0 is a fixed constant and independent of L. The total intensity is $I_{\mathrm{tot}} = \int du\, I(u) = I_0 L(1 + a\mathrm{sinc}n_1\pi)$. We multiply $K_{aa,bb}$ with the total intensity I_{tot} to obtain a total QFI $K'_{aa,bb}$ to take into account this effect in the numerical calculation; ignoring the correction factor when $n_{1,2}$ are not integers to get an intuitive interpretation, we have $K'_{aa,bb} \propto L^{-1}$, which indicates smaller sources result in larger QFI. This implies that we can increase the QFI by blocking part of the source on purpose. However, in terms of being a figure of merit for imaging quality, the QFI $K_{aa,bb}$ have the drawback of providing a bound that is not tight for multiparameter estimation problems, while imaging a general source requires estimating an infinite number of parameters [12,29,31]. Thus it is worth investigating further whether this strategy is actually useful in practice.

We plot the numerical calculation of the QFI $K_{aa,bb}$ in Fig. 5, where we fix the spatial frequency $k_{1,2}$ while varying the size of the source, i.e., varying α. As suggested above, besides oscillations, the QFI increases as α gets smaller. Intuitively, $\alpha =$ (size of source)/(resolution) and $n_{1,2} =$ (size of source)/(details' size). We would expect the largest QFI around $n_{1,2} \sim 1$. For the parameters chosen in Fig. 5, this corresponds to $\alpha/\pi \sim 0.1$, and we can indeed observe that the largest $K_{aa,bb}$ is obtained around $\alpha/\pi \sim 0.1$. We also present the result of the total QFI $K'_{aa,bb}$ after multiplying the QFI per photon $K_{aa,bb}$ with the total intensity. We can still observe an increase in $K'_{aa,bb}$ as α decreases, as promised in the above analytical discussion, but the increasing trend is much more gradual compared with $K_{aa,bb}$, which is also consistent with our analytical prediction.

The discussion above has focused on the estimation of a and b. Although we have argued that the spatial frequencies $k_{1,2}$ are known parameters based on the Whittaker-Shannon sampling theorem, it is not difficult to include $k_{1,2}$ as unknown parameters to estimate $k_{1,2}$, as an alternative approach. First we note that the state considered in Eq. (2) has only two degrees of freedom, i.e., the phase and amplitude of coherence function g, which means that we cannot estimate four independent parameters a, b, k_1, and k_2 simultaneously. However, we can use two pairs of telescopes with two different baselines to estimate the four parameters simultaneously, because in this case there are two independent coherence functions and four degrees of freedom. We give more detail about the estimation of $k_{1,2}$ in Appendix B.

III. PERFORMANCE OF A FIXED PHASE MEASUREMENT IN BANDWIDTH EXTRAPOLATION

The above discussion focused on the fundamental limit of estimating a and b, which is the best achievable sensitivity using any quantum measurement. Following the setup of Fig. 2, we now see how well the projective measurement onto the following state can do:

$$|\psi\rangle = \frac{1}{\sqrt{2}}(|0_A 1_B\rangle \pm e^{i\delta}|1_A 0_B\rangle). \tag{12}$$

Here δ is chosen as a fixed phase that has no particular relation to the coherence function, i.e., it deviates from the optimal choice, and $|0_A 1_B\rangle$ and $|1_A 0_B\rangle$ are the single-photon basis states of the two spatial modes of the two detectors. To quantify the performance of this measurement, we calculate the Fisher information [12]

$$F_{ij} = \sum_y \frac{1}{P(y|\vec{x})}\frac{\partial P(y|\vec{x})}{\partial x_i}\frac{\partial P(y|\vec{x})}{\partial x_j}, \tag{13}$$

where $P(y|\vec{x})$ is the probability of getting outcome y with a POVM $\{\Pi_y\}_y$ for a set of unknown parameters $\vec{x}$. The FI gives the bound of the variance of estimating unknown parameters with a chosen POVM and any unbiased estimator. The QFI is an upper bound of the FI since QFI is the result of optimizing FI over all possible POVMs: $\Sigma_{\vec{x}} \geqslant F^{-1} \geqslant K^{-1}$ [13,14].

Result 2: Performance of a fixed phase measurement in bandwidth extrapolation for a simple source

We find the FI of this measurement of estimating a and b to be

$$F_{aa} = \frac{A^2\cos^2(\delta+\phi)}{1-|g|^2\cos^2(\delta+\theta)},$$
$$F_{bb} = \frac{B^2\sin^2(\delta+\phi)}{1-|g|^2\cos^2(\delta+\theta)},$$
$$F_{ab} = \frac{-AB\sin(\delta+\phi)\cos(\delta+\phi)}{1-|g|^2\cos^2(\delta+\theta)}. \tag{14}$$

We first analyze the optimal choice of delay δ for two parameter regimes. The first corresponds to finite α where $|g|$ is usually very small. Alternatively, α may approach zero where $|g| \to 1$. In both case, we find the optimal choice of the phase delay δ approaches $\delta = -\phi$ for estimating a and $\delta = -\phi + \pi/2$ for estimating b. The FI of the two parameter regimes has different behaviors as δ deviates from the optimal values.

We numerically calculate the FI for the fixed phase estimation described in Eq. (12) and the QFI of estimating a and b using parameters $n_1 = 20$, $n_2 = 25$, $\phi = 0$, $a = 0.1$, and $b = 0.2$. For finite α, considering the denominator of the FI in Eq. (14), we find that $|g|^2\cos^2(\delta+\theta)$ is a small number for finite α and hence mainly the numerators of $F_{aa,bb}$ should be considered when choosing δ. It turns out that for an finite α and $\delta = -\phi = 0$, we have $FI_{aa}/K_{aa} \approx 1$ and $FI_{bb}/K_{bb} \approx 0$. This means $\delta = -\phi$ is close to the optimal measurement for estimating a. For $\delta = -\phi + \pi/2 = \pi/2$, we have $FI_{aa}/K_{aa} \approx 0$ and $FI_{bb}/K_{bb} \approx 1$. This means $\delta = -\phi + \pi/2$ is close to the optimal measurement for estimating b. For finite α, when δ deviates from its optimal values, we can read from Eq. (14) that the FI is only decreased by a constant factor. From Fig. 6, where we choose a phase delay deviating from the optimal values, we find that both F_{aa}/K_{aa} and F_{bb}/K_{bb} remain roughly $1/2$ for finite α.

When α approaches zero, i.e., $\alpha \to 0$, we have $|g| \to 1$, and then $|g|^2\cos^2(\delta+\theta)$ is no longer a smaller number. Notice that as $\alpha \to 0$, $A, B \to 0$, in which case $\theta \approx \phi$. One can easily verify that $\delta = -\phi$ and $\delta = -\phi + \pi/2$ are still the maximal points of $F_{aa,bb}$. However, when δ deviates from the optimal choice and is fixed at a constant value, the FI of estimating a is strongly affected since the denominator may deviate from zero and is very sensitive to the choice of phase δ. This is also shown in Fig. 6, where we fix $\delta = \pi/4$. The interesting part is the F_{aa}/K_{aa} close to $\alpha = 0$, where the vanishing F_{aa}/K_{aa} means the measurement performs much worse than the optimal sensitivity achievable with a physically allowed quantum measurement and hence implies there is much room for improvement of the measurement. This is expanded below as a discussion of limiting cases.

In the above discussion, we calculated the FI of a fixed phase measurement where we directly interfere the light received at the two spatial modes A and B after adding a phase delay. It turned out that a proper phase delay enables the optimal measurement and that any other phase delay is nonoptimal for the estimation of a and b. We also observed the different behaviors of performance for α approaching zero and finite α. We expand the discussion of these two

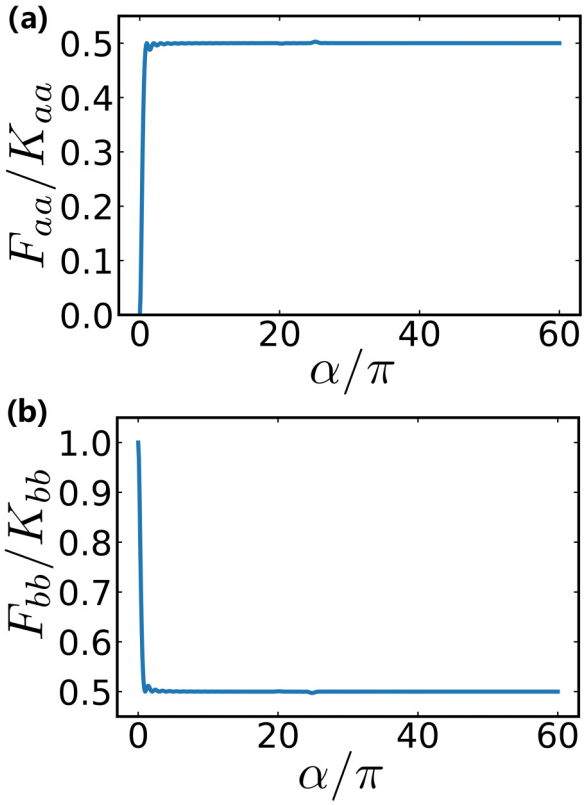

FIG. 6. Ratios between Fisher information and quantum Fisher information: (a) ratio F_{aa}/K_{aa} for the estimation of a and (b) ratio F_{bb}/K_{bb} for the estimation of b. We have chosen $\delta = \pi/4$, $n_1 = 20$, $n_2 = 25$, $\phi = 0$, $a = 0.1$, and $b = 0.2$.

parameter regimes by first looking at the limiting case when the whole size of the source L is very small compared to the resolution limit, i.e., $\alpha \to 0$. (In this case, since $n_{1,2}$ are nonzero, $\alpha \ll n_{1,2}\phi$.) Second, we consider finite α and assume the limiting case where the size of the source L is not small, i.e., $\alpha \sim O(1)$, but we want to measure some high-frequency component, i.e., $\alpha \ll n_{1,2}\pi$. This limit is of practical interest when it is desired to measure fine details of a large source below the resolution limit.

IV. SMALL-SOURCE LIMIT

We first consider the limiting case $\alpha \to 0$. The above results can be expanded as a series of α:

$$A \approx (-1)^{n_1+1}\frac{\alpha^2}{n_1^2\pi^2} + o(\alpha^2),$$
$$B \approx (-1)^{n_2+1}\frac{\alpha}{n_2\pi} + o(\alpha^2),$$
$$1-|g|^2 = \left(\frac{1}{3} + (-1)^{n_1}\frac{2}{n_1^2\pi^2}a - \frac{1}{n_2^2\pi^2}b^2\right)\alpha^2 + o(\alpha^2), \tag{15}$$
$$K_{aa} = \frac{\alpha^2}{n_1^4\pi^4\left[\frac{1}{3} + (-1)^{n_1}\frac{2a}{n_1^2\pi^2} - \frac{b^2}{n_2^2\pi^2}\right]} + o(\alpha^2),$$
$$K_{bb} = \frac{\alpha^2}{\pi^2\left[n_2^2 - \frac{3b^2n_1^2}{6(-1)^{n_1}a + n_1^2\pi^2}\right]} + o(\alpha^2). \tag{16}$$

From this result, we can clearly observe that as the size of the source becomes much smaller than the resolution limit, i.e., $\alpha \to 0$, the QFI of estimating both a and b vanishes, as shown in the bottom inset in Figs. 3(a) and 3(b). For the measurement with a fixed phase, i.e., the projection onto state $|\psi\rangle = \frac{1}{\sqrt{2}}(|0_A 1_B\rangle \pm e^{i\delta}|1_A 0_B\rangle)$, we find the FI of estimating a and b in this limit to be

$$F_{aa} = \frac{1}{n_1^4 \pi^4 \tan^2(\delta+\phi)}\alpha^4 + o(\alpha^4),$$
$$F_{bb} = \frac{1}{n_2^2\pi^2}\alpha^2 + o(\alpha^2). \tag{17}$$

Result 3: Performance improvement of bandwidth extrapolation

As $\alpha \to 0$, the ratio between the FI and QFI of estimating a and b is

$$F_{aa}/K_{aa} \propto \alpha^2 + o(\alpha^2),$$
$$F_{bb}/K_{bb} \propto 1 + o(1). \tag{18}$$

This means a carefully designed measurement can help improve the estimation of high-frequency information as $\alpha \to 0$.

To further understand this result, we consider how a and b are related to the amplitude $|g|$ and phase θ of the coherence function g,

$$|g| = 1 - \left(\frac{1}{6} + (-1)^{n_1}\frac{1}{n_1^2\pi^2}a - \frac{1}{2n_2^2\pi^2}b^2\right)\alpha^2 + o(\alpha^2), \tag{19}$$

$$\theta = \phi + b\frac{(-1)^{n_2+1}}{n_2\pi}\alpha + o(\alpha). \tag{20}$$

We emphasize that, to the second leading order of α, $|g|$ depends on both a and b, but θ depends on only b. This essentially leads to different behavior in the estimation of a and b. The reasons are clear with the calculation of the QFI and FI of estimating $|g|$ and θ, which we find to be

$$K_{|g||g|} = \frac{1}{1-|g|^2} = O(\alpha^{-2}),$$
$$K_{\theta\theta} = |g|^2 = O(1), \tag{21}$$
$$K_{|g|\theta} = 0.$$

As $\alpha \to 0$, we have $|g| \to 1$ and hence $K_{|g||g|} \to \infty$ and $K_{\theta\theta} \to 1$. The FI of estimating $|g|$ and θ with projective measurement onto state $|\psi\rangle = \frac{1}{\sqrt{2}}[1, \pm e^{i\delta}]^T/\sqrt{2}$ is

$$F_{|g||g|} = \frac{\cos^2(\theta-\delta)}{1-|g|^2\cos^2(\theta-\delta)},$$
$$F_{\theta\theta} = \frac{|g|^2\sin^2(\theta-\delta)}{1-|g|^2\cos^2(\theta-\delta)},$$
$$F_{\theta|g|} = -\frac{|g|\sin(\theta-\delta)\cos(\theta-\delta)}{1-|g|^2\cos^2(\theta-\delta)}. \tag{22}$$

We can see that we need $\delta \to \theta$ to have $F_{|g||g|} \to \infty$ and approaching $K_{|g||g|}$. Note $\theta = \arg g$ is an unknown parameter, so the measurement could be performed adaptively such that the phase δ in the measurement gradually approaches the optimal choice. If δ is arbitrarily chosen as a fixed number far from θ, we have $F_{|g||g|} \sim O(1)$. On the other hand, we need $\delta \to \theta + \pi/2$ to have $F_{\theta\theta}$ approaching $K_{\theta\theta}$. However, as long as θ is far from δ, $F_{\theta\theta} \sim O(1)$ is always true. In other words, in the limiting case $\alpha \to 0$, the estimation of $|g|$ strongly relies on the choice of δ and the estimation of θ is only slightly affected by the choice of δ. The QFI K and FI F with two set of unknown parameters $\vec{x}$ and $\vec{y}$ can be related to each other by [12–14]

$$K_{x_i x_j} = \sum_{k,l} K_{y_k y_l}\frac{\partial y_k}{\partial x_i}\frac{\partial y_l}{\partial x_j},$$
$$F_{x_i x_j} = \sum_{k,l} F_{y_k y_l}\frac{\partial y_k}{\partial x_i}\frac{\partial y_l}{\partial x_j}. \tag{23}$$

Notice that

$$\frac{\partial|g|}{\partial a} = (-1)^{n_1+1}\frac{1}{n_1^2\pi^2}\alpha^2 + o(\alpha^2),$$
$$\frac{\partial|g|}{\partial b} = \frac{b}{n_2^2\pi^2}\alpha^2 + o(\alpha^2),$$
$$\frac{\partial\theta}{\partial a} = o(\alpha),$$
$$\frac{\partial\theta}{\partial b} = (-1)^{n_2+1}\frac{1}{n_2\pi}\alpha + o(\alpha). \tag{24}$$

We can then observe the contribution of information from $|g|$ and θ to the estimation of a and b,

$$K_{aa} \sim K_{|g||g|}\left(\frac{\partial|g|}{\partial a}\right)^2 + K_{\theta\theta}\left(\frac{\partial\theta}{\partial a}\right)^2 \sim O(\alpha^2),$$
$$K_{|g||g|}\left(\frac{\partial|g|}{\partial a}\right)^2 \sim O(\alpha^{-2})O(\alpha^4) \sim O(\alpha^2),$$
$$K_{\theta\theta}\left(\frac{\partial\theta}{\partial a}\right)^2 \sim O(1)o(\alpha^2) \sim o(\alpha^2). \tag{25}$$

The sensitivity of estimating a is dominated by the information contained in $|g|$. However, in the case δ is arbitrarily chosen,

$$F_{aa} \sim F_{|g||g|}\left(\frac{\partial|g|}{\partial a}\right)^2 + F_{\theta\theta}\left(\frac{\partial\theta}{\partial a}\right)^2 + F_{\theta|g|}\frac{\partial\theta}{\partial a}\frac{\partial|g|}{\partial a} \sim o(\alpha^2),$$
$$F_{|g||g|}\left(\frac{\partial|g|}{\partial a}\right)^2 \sim O(1)O(\alpha^4) \sim o(\alpha^2),$$
$$F_{\theta\theta}\left(\frac{\partial\theta}{\partial a}\right)^2 \sim O(1)o(\alpha^2) \sim o(\alpha^2),$$
$$F_{\theta|g|}\frac{\partial\theta}{\partial a}\frac{\partial|g|}{\partial a} \sim O(1)o(\alpha^2) \sim o(\alpha^2). \tag{26}$$

So we cannot saturate the QFI of estimating a in this case. However, for the estimation of b,

$$K_{bb} \sim K_{|g||g|}\left(\frac{\partial|g|}{\partial b}\right)^2 + K_{\theta\theta}\left(\frac{\partial\theta}{\partial b}\right)^2 \sim O(\alpha^2),$$
$$K_{|g||g|}\left(\frac{\partial|g|}{\partial b}\right)^2 \sim O(\alpha^{-2})O(\alpha^4) \sim O(\alpha^2),$$
$$K_{\theta\theta}\left(\frac{\partial\theta}{\partial b}\right)^2 \sim O(1)O(\alpha^2) \sim O(\alpha^2). \tag{27}$$

Different from the estimation a, both $|g|$ and θ contribute a comparable amount of information to the estimation of b. Again, if δ is arbitrarily chosen,

$$\begin{aligned} F_{bb} &\sim F_{|g||g|}\left(\frac{\partial|g|}{\partial b}\right)^2 + F_{\theta\theta}\left(\frac{\partial\theta}{\partial b}\right)^2 + F_{\theta|g|}\frac{\partial\theta}{\partial a}\frac{\partial|g|}{\partial a} \\ &\sim O(\alpha^2), \\ F_{|g||g|}\left(\frac{\partial|g|}{\partial b}\right)^2 &\sim O(1)O(\alpha^4) \sim o(\alpha^2), \\ F_{\theta\theta}\left(\frac{\partial\theta}{\partial b}\right)^2 &\sim O(1)O(\alpha^2) \sim O(\alpha^2), \\ F_{\theta|g|}\frac{\partial\theta}{\partial a}\frac{\partial|g|}{\partial a} &= O(1)O(\alpha^3) \sim o(\alpha^2). \end{aligned} \tag{28}$$

Because the sensitivity of estimating θ is not affected much by a randomly chosen δ deviating from the optimal value, we can have FI which is of the same order of α as the QFI in the estimation of b. This explains the results in Eqs. (16) and (17): The significant improvement of bandwidth extrapolation in the small limit is related to the increasing of sensitivity of estimating $|g|$ as $|g| \to 1$.

V. FINE DETAILS OF A FINITE-SIZE SOURCE

Now we consider the other limiting case, when $\alpha \sim O(1)$ and $n_1, n_2 \to \infty$. This corresponds to the case when the size of the source is larger than the resolution limit of the interferometer, but we want to estimate the fine details of the source that are below the resolution limit. In this case, $1 - |g|^2$ is a nonvanishing constant factor of $O(1)$,

$$\begin{aligned} A &\approx (-1)^{n_1+1}\frac{\alpha\sin\alpha}{n_1^2\pi^2} + o\big(n_1^{-2}\big), \\ B &\approx (-1)^{n_2+1}\frac{\sin\alpha}{n_2\pi} + o\big(n_2^{-1}\big). \end{aligned} \tag{29}$$

In this case, the QFI can be expanded as a series in n_1 and n_2 and Eq. (11) becomes

$$\begin{aligned} K_{aa} &\approx \frac{\alpha^2\sin^2\alpha}{(1-|g|^2)n_1^4\pi^4} + o\big(n_1^{-4}\big), \\ K_{bb} &\approx \frac{\sin^2\alpha}{n_2^2\pi^2} + o\big(n_2^{-2}\big). \end{aligned} \tag{30}$$

For the measurement with a fixed phase, the FI is given as

$$\begin{aligned} F_{aa} &\approx \frac{\cos^2(\delta+\phi)\alpha^2\sin^2\alpha}{[1-|g|^2\cos^2(\theta+\delta)]n_1^4\pi^4} + o\big(n_1^{-4}\big), \\ F_{bb} &\approx \frac{\sin^2(\delta+\phi)}{1-|g|^2\cos^2(\theta+\delta)}\frac{\sin^2\alpha}{n_2^2\pi^2} + o\big(n_2^{-2}\big). \end{aligned} \tag{31}$$

We can see now that the more carefully designed measurement and the measurement with a fixed phase have similar scaling as a function of n_1 and n_2, which suggests the more carefully designed measurement will not provide an obvious advantage.

VI. QUANTUM-METROLOGY-INSPIRED METHODS FROM THE PERSPECTIVE OF BANDWIDTH EXTRAPOLATION

We now briefly reinterpret quantum-metrology-inspired methods based on the ideas from bandwidth extrapolation by considering a simple example. We consider the simple case where we have two weak monochromatic point sources in one dimension at positions u_1 and u_2, respectively, and we want to measure the separation $\Delta u = u_2 - u_1$ and the centroid $\bar{u} = (u_1 + u_2)/2$ with an interferometer that has two detectors with baseline d. The density matrix of the state received by the two detectors is still described by Eq. (2) but with

$$g = (e^{i\phi_1} + e^{i\phi_2})/2, \quad \phi_{1,2} = \frac{\omega}{c}\frac{u_{1,2}d}{z_0}. \tag{32}$$

Notice the centroid information $\bar{u}$ is only contained in the phase θ of g and the separation information Δu is only contained in the amplitude $|g|$.

As discussed in [19,32], the QFI of estimating the separation Δu and centroid $\bar{u}$ is calculated as

$$\begin{aligned} K_{\bar{u}\bar{u}} &= \frac{\omega^2 d^2}{c^2 z_0^2}\cos^2\frac{\phi_1-\phi_2}{2}, \\ K_{\Delta u\Delta u} &= \frac{\omega^2 d^2}{4c^2 z_0^2}, \\ K_{\bar{u}\Delta u} &= 0. \end{aligned} \tag{33}$$

In the limit of $\Delta u \to 0$, we have nonvanishing QFI $K_{\Delta u\Delta u} = \frac{\omega^2 d^2}{4c^2 z_0^2}$ of estimating Δu, which is referred to as superresolution. It is interesting to observe that this is equivalent to saturating the QFI of estimating $|g|$ and θ, which is given in Eq. (21) as

$$K_{\Delta u\Delta u} = K_{|g||g|}\left(\frac{\partial|g|}{\Delta u}\right)^2. \tag{34}$$

As $\Delta u \to 0$, the two factors have different behaviors,

$$\begin{aligned} K_{|g||g|} &= \frac{1}{\frac{1}{4}\frac{\omega^2 d^2}{c^2 z_0^2}\Delta u^2 + o(\Delta u^2)} \to \infty, \\ \left(\frac{\partial|g|}{\Delta u}\right)^2 &= \frac{1}{16}\frac{w^4 d^4}{c^4 z_0^4}\Delta u^2 + o(\Delta u^2) \to 0, \end{aligned} \tag{35}$$

which cancel out exactly and give us a constant $K_{\Delta u\Delta u}$. The measurement used to saturate both $K_{\Delta u\Delta u}$ and $K_{|g||g|}$ is the projective measurement onto state

$$\frac{1}{\sqrt{2}}(|01\rangle \pm e^{-i\delta}|10\rangle), \quad \delta = \frac{\phi_1+\phi_2}{2}. \tag{36}$$

Note that prior knowledge of $\phi_1 + \phi_2$ is needed to implement this optimal measurement, which can be achieved by doing the measurement adaptively. More generally speaking, the QFI of estimating any set of parameters can be directly derived from the QFI of estimating $\{g_{ij}\}$ of the received states by a transformation [12–14]. If we can construct a POVM which saturates the QFI of $\{g_{ij}\}$, then this POVM automatically is optimal for any set of parameters. In a nonrigorous sense, we can

say that improving the estimation of lower-frequency information is the root of any miracle in quantum-metrology-inspired methods. This claim is nonrigorous because we usually cannot have a POVM which saturates the QFI for all parameters in a multiparameter estimation problem due to the incompatibility of optimal measurements of different parameters, which is a nontrivial aspect worth further discussion.

VII. CONCLUSION

In summary, we have discussed the relation between bandwidth extrapolation and quantum-metrology-inspired methods in interferometric imaging. We first calculated the fundamental sensitivity limit of estimating two Fourier components of a spatially bound source using an interferometer with two detectors. The QFI calculation illuminates the difficulties of the bandwidth extrapolation method. The measurement with an arbitrary fixed phase can saturate the fundamental imaging resolution limit except for the case when $\alpha \to 0$, i.e., when the source size is much smaller than the conventional resolution limit of the imaging system. In the case of $\alpha \to 0$, a more carefully designed measurement can significantly improve the sensitivity. This is also the limit adopted by most previous discussions on quantum-metrology-inspired methods. We also paid attention to another important limiting case of when $\alpha \sim O(1)$ and $n_{1,2}\pi \gg 1$, which means the size of the source is not small but we care about the fine details of the source that are below the resolution limit, and found that a carefully designed measurement will not help much. We also reinterpreted quantum-metrology-inspired methods from the perspective of bandwidth extrapolation to find that for a spatially bounded source, information can be obtained about its fine details from the accessible low-frequency information.

ACKNOWLEDGMENTS

We are especially grateful to Yujie Zhang for valuable feedback and comments. We also thank Eric Chitambar, Andrew Jordan, Paul Kwiat, John D. Monnier, Shayan Mookherjea, Michael G. Raymer, and Brian J. Smith for helpful discussions. This work was supported by the multiuniversity National Science Foundation Grant No. 1936321, QII-TAQS: Quantum-Enhanced Telescopy.

APPENDIX A: WHITTAKER-SHANNON SAMPLING THEOREM FOR SPATIALLY BOUNDED SOURCES

We have emphasized that one consequence of having a spatially bounded source is the possibility to do bandwidth extrapolation. However, there is another consequence of spatially bounded $I(u)$, namely, that we only need to measure a discrete set of spatial Fourier components $\{g(\alpha_n)\}_n$ to know the continuous function of the spatial spectrum $g(\alpha)$, where we have explicitly written the dependence of g on $\alpha = \frac{dL\omega}{2cz_0}$. This is a direct result of the Whittaker-Shannon sampling theorem [4]. Here we rederive it with our notation for completeness.

Assume we measure only a discrete set of Fourier components and get a sampled function

$$\begin{aligned} g_s(\alpha) &= g(\alpha)\mathrm{comb}(\alpha), \\ \mathrm{comb}(\alpha) &= \alpha_0 \sum_{n=-\infty}^{\infty} \delta(\alpha - n\alpha_0), \end{aligned} \tag{A1}$$

where $g(\alpha)$ is the original coherence function and $g_s(\alpha)$ samples points equally spaced with separation α_0. Our goal is to prove that when the separation α_0 is chosen to be small enough and the source is spatially bounded to be within $-L/2 \leqslant u \leqslant L/2$, $g_s(\alpha)$ can be used to exactly construct $g(\alpha)$. We will also prove that in this case, without losing any information, we can assume that the intensity distribution $I(u)$ has the form of

$$\begin{aligned} I(u) &= \left(\frac{1}{L} + \frac{1}{L}\sum_{n=1}^{\infty} a_n \cos k_n u + \frac{1}{L}\sum_{n=1}^{\infty} b_n \sin k_n u\right)\mathrm{rect}(u), \\ \mathrm{rect}(u) &= \begin{cases} 1 & \text{for } -\frac{L}{2} \leqslant u \leqslant \frac{L}{2} \\ 0 & \text{otherwise,} \end{cases} \end{aligned} \tag{A2}$$

where $k_n = 2n\pi/L$ are known and a_n and b_n are the unknown parameters we need to estimate.

We can easily check that the inverse Fourier transformation of $g(\alpha)$ defined in Eq. (4) gives the intensity distribution of the source $I(u)$,

$$\mathcal{F}^{-1}(g(\alpha))(u) = \int d\alpha\, g(\alpha) e^{-i(2u/L)\alpha} = \pi L I(u), \tag{A3}$$

where we assume that $I(u)$ is any general function which is spatially bounded. Let us calculate the inverse Fourier transformation of sampled $g_s(\alpha)$,

$$\begin{aligned} \mathcal{F}^{-1}(g_s(\alpha))(u) &= \int d\alpha\, g_s(\alpha) e^{-i(2u/L)\alpha} \\ &= \pi L \sum_{n=-\infty}^{+\infty} I\left(u - n\pi\frac{L}{\alpha_0}\right). \end{aligned} \tag{A4}$$

We can observe that $\mathcal{F}^{-1}(g_s(\alpha))(u)$ is simply the sum of $I(u)$ shifted by $n\pi\frac{L}{\alpha_0}$. Recall that the source is spatially bounded be within $-L/2 \leqslant u \leqslant L/2$. If we can choose α_0 to be small enough such that

$$\pi\frac{L}{\alpha_0} \geqslant L, \tag{A5}$$

there is no overlap between each term of the sum in Eq. (A4). Define

$$\mathrm{rect}_2(u) = \begin{cases} 1 & \text{for } -\frac{\pi L}{2\alpha_0} \leqslant u \leqslant \frac{\pi L}{2\alpha_0} \\ 0 & \text{otherwise.} \end{cases} \tag{A6}$$

It is obvious that as long as $\pi\frac{L}{\alpha_0} \geqslant L$, we have

$$[\mathcal{F}^{-1}(g_s(\alpha))(u)]\mathrm{rect}_2(u) = \mathcal{F}^{-1}(g(\alpha))(u) = \pi L I(u). \tag{A7}$$

Let us further do a Fourier transformation on both sides of Eq. (A7), which gives

$$g(\alpha) = \sum_{n=-\infty}^{+\infty} g(n\alpha_0)\mathrm{sinc}\frac{(\alpha - n\alpha_0)\pi}{\alpha_0}. \tag{A8}$$

This means that as long as $\pi\frac{L}{\alpha_0} \geqslant L$, we can reconstruct the whole spatial spectrum $g(\alpha)$ with the discrete set of points $\{g(n\alpha_0)\}_n$. This is one possible form of Whittaker-Shannon sampling theorem.

Now we prove that for any spatially bounded $I(u)$, we can always rewrite it as Eq. (A2) without losing any information. If we use the form of $g_s(\alpha)$ in Eq. (A1) to calculate its inverse Fourier transformation,

$$\begin{aligned}&\mathcal{F}^{-1}(g_s(\alpha))(u)\\&= \alpha_0 g(0) + \sum_{n=1}^{\infty}\alpha_0[g(n\alpha_0)+g(-n\alpha_0)]\cos\frac{2u}{L}n\alpha_0\\&\quad + i\sum_{n=1}^{\infty}\alpha_0[-g(n\alpha_0)+g(-n\alpha_0)]\sin\frac{2u}{L}n\alpha_0,\end{aligned} \tag{A9}$$

we then get a form of the intensity distribution under the condition $\pi\frac{L}{\alpha_0} \geqslant L$ based on Eq. (A7):

$$\begin{aligned}I(u) = \frac{\alpha_0}{\pi L}\Bigg(&g(0) + \sum_{n=1}^{\infty}[g(n\alpha_0)+g(-n\alpha_0)]\cos\frac{2u}{L}n\alpha_0\\&+ i\sum_{n=1}^{\infty}[-g(n\alpha_0)+g(-n\alpha_0)]\sin\frac{2u}{L}n\alpha_0\Bigg)\mathrm{rect}_2(u).\end{aligned} \tag{A10}$$

For simplicity, let us assume that $\pi/\alpha_0 = 1$, which is the maximal α_0 satisfying $\pi\frac{L}{\alpha_0} \geqslant L$. We define

$$a_n = g(n\pi)+g(-n\pi), \quad b_n = i[-g(n\pi)+g(-n\pi)]. \tag{A11}$$

We can then get the intensity distribution in Eq. (A2) as promised. It is easy to check that a_n and b_n are real numbers based on the definition of $g(\alpha)$. In the above derivation, we can easily find that k_n is actually determined by our choice of sampled points $\{\alpha_n\}_n$, which means k_n are known parameters. Notice Eq. (A2) is one possible form of intensity distribution which can represent a general spatially bounded source. We have the freedom to choose another discrete set of $\{g(\alpha_n)\}_n$ which will give different forms of $I(u)$. However, in general, as long as we choose a discrete set of $\{g(\alpha_n)\}_n$ that is dense enough, we will not lose any information.

APPENDIX B: ESTIMATION OF $k_{1,2}$

If we treat the spatial frequencies $k_{1,2}$ in Eq. (1) as unknown parameters, we can calculate the QFI matrix for the estimation of all four parameters a, b, k_1, and k_2 to quantify the performance. If we still consider the setup in Fig. 2, we can exploit the relations

$$\frac{\partial\rho}{\partial k_1} = \frac{a}{A}\frac{\partial A}{\partial k_1}\frac{\partial\rho}{\partial a}, \quad \frac{\partial\rho}{\partial k_2} = \frac{b}{B}\frac{\partial B}{\partial k_2}\frac{\partial\rho}{\partial b}, \tag{B1}$$

where ρ is the single-photon state given in Eq. (2). These relations immediately tell us that the QFI matrix for the estimation of all four parameters is

$$\begin{aligned}K &= MK'M,\\K &= \begin{bmatrix}K_{aa} & K_{ab} & K_{ak_1} & K_{ak_2}\\K_{ba} & K_{bb} & K_{bk_1} & K_{bk_2}\\K_{k_1a} & K_{k_1b} & K_{k_1k_1} & K_{k_1k_2}\\K_{k_2a} & K_{k_2b} & K_{k_2k_1} & K_{k_2k_2}\end{bmatrix},\\M &= \begin{bmatrix}1 & 0 & 0 & 0\\0 & 1 & 0 & 0\\0 & 0 & \frac{a}{A}\frac{\partial A}{\partial k_1} & 0\\0 & 0 & 0 & \frac{b}{B}\frac{\partial B}{\partial k_2}\end{bmatrix},\\K' &= \begin{bmatrix}K_{aa} & K_{ab} & K_{aa} & K_{ab}\\K_{ba} & K_{bb} & K_{ba} & K_{bb}\\K_{aa} & K_{ab} & K_{aa} & K_{ab}\\K_{ba} & K_{bb} & K_{ba} & K_{bb}\end{bmatrix},\end{aligned} \tag{B2}$$

where K_{aa}, K_{ab}, and K_{bb} are given in Eq. (11). Notice K and K' are not full rank. This means we cannot estimate all four parameters simultaneously. Intuitively, the state in Eq. (2) has only two degrees of freedom, namely, the phase and amplitude of the coherence function g. We will be unable to estimate four independent unknown parameters.

There is a simple solution for this problem. We can use two baselines to estimate all four parameters a, b, k_1, and k_2. Assume we have two pair of telescopes with different baselines $d_{1,2}$, respectively, and each pair of telescopes receives a photon from a source with intensity distribution given in Eq. (1). The state received by the two pairs of telescopes can be written as

$$\begin{aligned}\rho_1\otimes\rho_2 &= \frac{1}{2}\begin{bmatrix}1 & g_1\\g_1^* & 1\end{bmatrix}\otimes\frac{1}{2}\begin{bmatrix}1 & g_2\\g_2^* & 1\end{bmatrix},\\g_1 &= e^{i\phi_1}(\mathrm{sinc}\alpha_1 + A_1a + iB_1b),\\g_2 &= e^{i\phi_2}(\mathrm{sinc}\alpha_2 + A_2a + iB_2b),\\\phi_{1,2} &= \frac{\omega}{c}\frac{u_0d_{1,2}}{z_0}, \quad \alpha_{1,2} = \frac{d_{1,2}L\omega}{2cz_0},\\A_{1,2} &= \frac{1}{2}[\mathrm{sinc}(\alpha_{1,2}-n_1\pi)+\mathrm{sinc}(\alpha_{1,2}+n_1\pi)],\\B_{1,2} &= \frac{1}{2}[\mathrm{sinc}(\alpha_{1,2}-n_1\pi)-\mathrm{sinc}(\alpha_{1,2}+n_1\pi)].\end{aligned} \tag{B3}$$

In this case, we have two independent $g_{1,2}$ which contain four degrees of freedom and hence we can expect to estimate all four parameters simultaneously. We can again try to explore the relations between derivatives over different parameters:

$$\begin{aligned}\frac{\partial\rho_1\otimes\rho_2}{\partial a} &= \frac{\partial\rho_1}{\partial a}\otimes\rho_2 + \rho_1\otimes\frac{\partial\rho_2}{\partial a},\\\frac{\partial\rho_1\otimes\rho_2}{\partial b} &= \frac{\partial\rho_1}{\partial b}\otimes\rho_2 + \rho_1\otimes\frac{\partial\rho_2}{\partial b},\\\frac{\partial\rho_1\otimes\rho_2}{\partial k_1} &= \frac{a}{A_1}\frac{\partial A_1}{\partial k_1}\left(\frac{\partial\rho_1}{\partial a}\otimes\rho_2\right) + \frac{a}{A_2}\frac{\partial A_2}{\partial k_1}\left(\rho_1\otimes\frac{\partial\rho_2}{\partial a}\right),\\\frac{\partial\rho_1\otimes\rho_2}{\partial k_2} &= \frac{b}{B_1}\frac{\partial B_1}{\partial k_2}\left(\frac{\partial\rho_1}{\partial b}\otimes\rho_2\right) + \frac{b}{B_2}\frac{\partial B_2}{\partial k_2}\left(\rho_1\otimes\frac{\partial\rho_2}{\partial b}\right).\end{aligned} \tag{B4}$$

Unlike the case when we only have one pair of telescopes, the derivative over $n_{1,2}$ is no longer proportional to the derivative over a and b. Indeed, we calculate out each element of the QFI matrix and find its determinant to be

$$\det K = \frac{16\pi^4 a^2 b^2 \left(A_2 \frac{\partial A_1}{\partial k_1} - A_1 \frac{\partial A_2}{\partial k_1}\right)^2 \left(B_2 \frac{\partial B_1}{\partial k_2} - B_1 \frac{\partial B_2}{\partial k_2}\right)^2}{L^4 (1 - |g_1|^2)(1 - |g_2|^2)}. \tag{B5}$$

As long as the baselines are unequal $d_1 \neq d_2$, we have $\det K \neq 0$. This means that we can estimate all four parameters a, b, k_1, and k_2 simultaneously. In the actual implementation of interferometric imaging, we usually sample many Fourier components using different baselines. So it is reasonable to expect that we are able to use more than one pair of telescopes in the estimation.

[1] J. L. Harris, Diffraction and resolving power, J. Opt. Soc. Am. **54**, 931 (1964).

[2] C. W. Barnes, Object restoration in a diffraction-limited imaging system, J. Opt. Soc. Am. **56**, 575 (1966).

[3] B. R. Frieden, Band-unlimited reconstruction of optical objects and spectra, J. Opt. Soc. Am. **57**, 1013 (1967).

[4] J. W. Goodman, *Introduction to Fourier Optics* (Roberts, Boston, 2005).

[5] E. J. Candès and C. Fernandez-Granda, Towards a mathematical theory of super-resolution, Commun. Pure Appl. Math. **67**, 906 (2014).

[6] R. Gerchberg, Super-resolution through error energy reduction, Opt. Acta **21**, 709 (1974).

[7] A. Papoulis, A new algorithm in spectral analysis and band-limited extrapolation, IEEE Trans. Circuits Syst. **22**, 735 (1975).

[8] C. Rushforth and R. Harris, Restoration, resolution, and noise, J. Opt. Soc. Am. **58**, 539 (1968).

[9] P. Sementilli, B. R. Hunt, and M. Nadar, Analysis of the limit to superresolution in incoherent imaging, J. Opt. Soc. Am. A **10**, 2265 (1993).

[10] M. Tsang, R. Nair, and X.-M. Lu, Quantum Theory of Superresolution for Two Incoherent Optical Point Sources, Phys. Rev. X **6**, 031033 (2016).

[11] M. Tsang, Resolving starlight: A quantum perspective, Contemp. Phys. **60**, 279 (2019).

[12] C. Helstrom, *Quantum Detection and Estimation Theory* (Academic, New York, 1976).

[13] S. L. Braunstein and C. M. Caves, Statistical Distance and the Geometry of Quantum States, Phys. Rev. Lett. **72**, 3439 (1994).

[14] M. G. Paris, Quantum estimation for quantum technology, Int. J. Quantum Inf. **07**, 125 (2009).

[15] C. Lupo and S. Pirandola, Ultimate Precision Bound of Quantum and Subwavelength Imaging, Phys. Rev. Lett. **117**, 190802 (2016).

[16] R. Nair and M. Tsang, Far-Field Superresolution of Thermal Electromagnetic Sources at the Quantum Limit, Phys. Rev. Lett. **117**, 190801 (2016).

[17] J. Řehaček, Z. Hradil, B. Stoklasa, M. Paúr, J. Grover, A. Krzic, and L. L. Sánchez-Soto, Multiparameter quantum metrology of incoherent point sources: Towards realistic superresolution, Phys. Rev. A **96**, 062107 (2017).

[18] J. Řeháček, Z. Hradil, D. Koutný, J. Grover, A. Krzic, and L. L. Sánchez-Soto, Optimal measurements for quantum spatial superresolution, Phys. Rev. A **98**, 012103 (2018).

[19] Y. Wang, Y. Zhang, and V. O. Lorenz, Superresolution in interferometric imaging of strong thermal sources, Phys. Rev. A **104**, 022613 (2021).

[20] S. Z. Ang, R. Nair, and M. Tsang, Quantum limit for two-dimensional resolution of two incoherent optical point sources, Phys. Rev. A **95**, 063847 (2017).

[21] Z. Yu and S. Prasad, Quantum Limited Superresolution of an Incoherent Source Pair in Three Dimensions, Phys. Rev. Lett. **121**, 180504 (2018).

[22] C. Napoli, S. Piano, R. Leach, G. Adesso, and T. Tufarelli, Towards Superresolution Surface Metrology: Quantum Estimation of Angular and Axial Separations, Phys. Rev. Lett. **122**, 140505 (2019).

[23] S. Prasad and Z. Yu, Quantum-limited superlocalization and superresolution of a source pair in three dimensions, Phys. Rev. A **99**, 022116 (2019).

[24] M. Tsang, Subdiffraction incoherent optical imaging via spatial-mode demultiplexing, New J. Phys. **19**, 023054 (2017).

[25] S. Zhou and L. Jiang, Modern description of Rayleigh's criterion, Phys. Rev. A **99**, 013808 (2019).

[26] M. Tsang, Quantum limit to subdiffraction incoherent optical imaging, Phys. Rev. A **99**, 012305 (2019).

[27] M. Tsang, Quantum Nonlocality in Weak-Thermal-Light Interferometry, Phys. Rev. Lett. **107**, 270402 (2011).

[28] F. Zernike, The concept of degree of coherence and its application to optical problems, Physica **5**, 785 (1938).

[29] S. Ragy, M. Jarzyna, and R. Demkowicz-Dobrzański, Compatibility in multiparameter quantum metrology, Phys. Rev. A **94**, 052108 (2016).

[30] J. Yang, S. Pang, Y. Zhou, and A. N. Jordan, Optimal measurements for quantum multiparameter estimation with general states, Phys. Rev. A **100**, 032104 (2019).

[31] A. S. Holevo, *Probabilistic and Statistical Aspects of Quantum Theory* (North-Holland, Amsterdam, 1982).

[32] C. Lupo, Z. Huang, and P. Kok, Quantum Limits to Incoherent Imaging are Achieved by Linear Interferometry, Phys. Rev. Lett. **124**, 080503 (2020).